

Implementation of expressions using Python in stimulated luminescence analysis

K. Prevezanou^{a,*}, G. Kioselaki^a, E. Tsoutsoumanos^{b,c}, P.G. Konstantinidis^a, G.S. Polymeris^c, V. Pagonis^d, G. Kitis^a

^a Aristotle University of Thessaloniki, Physics Department, Nuclear Physics and Elementary Particles Physics Section, GR-54124, Thessaloniki, Greece

^b Condensed Matter Physics Laboratory, Physics Department, University of Thessaly, GR-35100, Lamia, Greece

^c Institute of Nanoscience and Nanotechnology, NCSR "Demokritos", GR-15310, Ag. Paraskevi (Athens), Greece

^d McDaniel College, Physics Department, Westminster, MD 21157, USA

ARTICLE INFO

Keywords:

Stimulated luminescence
Deconvolution
Dose response
Python
Lambert W

ABSTRACT

In Thermoluminescence (TL) and Optically Stimulated Luminescence (OSL), the study of complex experimental TL glow curves and OSL signal processing, also known as deconvolution, was revolutionized by using a single, analytic master equation described by Lambert W function. This latter equation has been also adopted for the case of dose response fitting. The present study exploits the utilization of Lambert W function in Python programming environment. These analytic expressions are based on One Trap-One Recombination center (OTOR) and Two Traps-One Recombination center (TTOR) models. Python scripts, with corresponding software flowchart being described in general, are created to deconvolve TL, LM-OSL, CW-OSL as well as to fit dose response experimental data. The calculated results are in agreement with those of the existing literature. Also, all scripts are free and available in GitHub to the research community for downloading.

1. Introduction

Mathematical formulation of stimulated luminescence phenomena has always been an interesting, albeit difficult research topic. This topic includes multiple tasks, such as the deconvolution of various curves indicating overlapping of components, fitting of dose response curves, simulation approaches of various aspects of stimulated luminescence, etc. This former statement is even more accurate especially for the case of Thermoluminescence (TL), since the differential equations of the effect were initially solved using arithmetical assumptions (Kitis et al., 1998). The computerized glow curve deconvolution (CGCD) analysis technique has been recognized as the strongest tool available for treating experimental glow curves of TL. Various physical single peak models are available for the description of single glow curves components; for a review on these models, the reader could refer to Kitis et al. (2019) and Konstantinidis et al. (2021). The use of Lambert W function in the description of stimulated luminescence has highly improved the deconvolution analysis technique. Earlier, Kitis and Vlachos (2013) and Singh and Gartia (2013) have demonstrated that this function could be used in order to construct an analytic solution for the differential equations that govern Thermoluminescence. Later on, these equations were transformed so that to include practical fitting parameters, such as the maximum intensity (I_m) and the temperature corresponding to this

(T_m) (Sadek et al., 2014b,a). In a recent review article, Kitis et al. (2019) have reported that the use of Lambert W function enables a single master equation for the description of the entire spectrum of stimulated luminescence curves, including TL, Optically Stimulated Luminescence (OSL) as well as isothermal TL.

Moreover, the dose response curves require fitting analysis; in many cases these were fitted using empirical equations, namely linear, saturating exponential or even a combination of those aforementioned equations. In another expression, the luminescence intensity is related to the μ -power dependence of the dose. The coefficient μ being the main fitting parameter of interest, is also named as the linearity coefficient, as it indicates important information regarding supra- or sub-linear behavior of the dose response. Pagonis et al. (2020a) and Pagonis et al. (2020b) have exploited the use of Lambert W function in an effort to fit the dose response curves using analytic expressions that are much more physically meaningful. This equation provides a simpler interpretation of the shape of the dose response curve than the empirical μ -power dependence of the dose, for many types of materials and for TL, OSL and ESR signals, as it contains physically meaningful parameters that provide information on the physical mechanism governing the behavior of the dose response data. Moreover, this new approach

* Corresponding author.

E-mail address: kpreveza@physics.auth.gr (K. Prevezanou).

was proven to be much more efficient, not to mention successful, in cases where severe supra-linearity takes place. Nevertheless, possible luminescence age limit extensions along with improving the accuracy of the calibration of luminescence dose response beyond its linear region, namely close to the saturation points, stand among the most important possible outcomes of this latter approach.

Regardless whether Lambert W function is being used either for deconvolving luminescence signals or fitting dose response curves, R stands as the most important fitting parameter; it corresponds to the ratio of the re-trapping over the recombination coefficients, and indicates the order of kinetics. The significance of such parameter is similar to the significance of the b parameter in the GOK model, representing the parameter that identifies the order of kinetics. Thus, in general, it takes values ranging between 0 and 1, with the first value corresponds to negligible re-trapping and first order of kinetics, while the later value indicates significant re-trapping and second order of kinetics (Kitis and Vlachos, 2013).

The use of Lambert W function in either deconvolution of stimulated luminescence curves or fitting of dose response curves requires excessive exertion. Even for the case of the most widely spread commercially available software such as Excel, this equation is not a built-in a function; thus it requires an implementation to the software. Konstantinidis et al. (2021) have recently reported on such implementation of Lambert W. The present work follows on directly from this latter aforementioned citation, aiming to describe the contribution of Lambert W function in a computing environment developed in Python to the (a) deconvolution of stimulated luminescence curves and (b) fitting experimental dose response curves. In terms of software development, R (Pagonis, 2021) and Python stand out as the two most often used programming languages for stimulated luminescence analysis, and are even included in many commercially available luminescence readers as part of their computational software. Since Lambert W function, and its equivalent Wright Omega function (Singh and Gartia, 2015), are already built-in to Python's library SciPy, an implementation for any of those functions is not further required, so they can be automatically imported in the form of a command. Additionally, the entire analysis is being presented in the form of open-source scripts that are being uploaded to GitHub, being available to the entire luminescence community not only for use, but for any possible further improvement by researchers that are willing to contribute. Finally, in order to establish the credibility of the analysis, the results of the present study are compared to (a) the corresponding results using the software by Konstantinidis et al. (2021) and (b) the corresponding results using the General Order Kinetic (GOK) model in the commercially available environment of Afouxenidis et al. (2011).

2. Analytic expressions for software development

The software development for CGCD analysis of complex stimulated luminescence curves requires analytic equations for the single component of each stimulation mode. The analytic single component model used is of physical basis because it was obtained from the analytic solution of the One Trap One Recombination center model (OTOR) shown in Fig. 1 (Kitis and Vlachos, 2013). In the OTOR model, the transition results to the creation of the electron-hole pairs. A_n (cm^3s^{-1}) and A_m (cm^3s^{-1}) are the re-trapping and recombination coefficients. In this case, N (cm^{-3}) and n (cm^{-3}) are the concentrations of the available electron traps and of the electrons trapped in N, while M (cm^{-3}) and m (cm^{-3}) represent the same concentrations for the holes. The analytic solution of the OTOR model provides a core equation which is the same for all stimulated luminescence phenomena, named as 'master equation'. Before the script description, the expressions used are displayed below for the cases of TL, Linearly Modulated OSL (LM-OSL) and Continuous Wave OSL (CW-OSL):

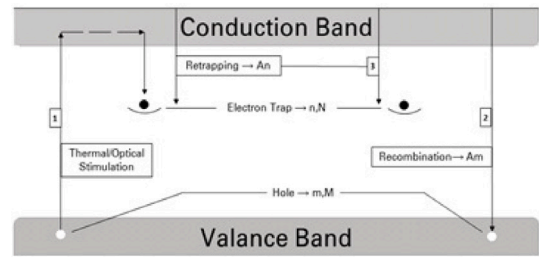


Fig. 1. Schematic diagram of the stimulation, recombination and re-trapping stages in the framework of the OTOR model.

2.1. Analytic equations for TL glow peak

TL equations

$$I(I_m, T_m, E, R, T) = I_m \exp\left(\frac{E(T - T_m)}{KTT_m}\right) \frac{W(e^{z_m}) + W(e^{z_m})^2}{W(e^z) + W(e^z)^2} \quad (1)$$

$$z = \frac{R}{1-R} - \ln\left(\frac{1-R}{R}\right) + \frac{E \exp(E/KT_m)}{KT_m^2} \frac{F(T, E)}{1 - 1.05R^{1.26}} \quad (2)$$

$$F(T, E) = T \exp(-E/KT) + \frac{E}{K} \cdot Ei(-E/KT) \quad (3)$$

where I_m is the maximum TL intensity, T_m the temperature at I_m , E the activation energy, $-Ei(-x) = E \int_x^\infty \frac{e^{-x}}{x} dx$ the exponential integral and R the re-trapping to recombination probabilities ratio.

2.2. Analytic equations for LM-OSL component

LM-OSL equations

$$I_m = \frac{t \cdot I_m \lambda}{I_m} \frac{W(e^{z_m}) + W(e^{z_m})^2}{W(e^z) + W(e^z)^2} \quad (4)$$

$$z = \frac{R}{1-R} - \ln\left(\frac{1-R}{R}\right) + \frac{t^2}{I_m^2} \frac{1}{(1-R)(1 + 0.534156 \cdot R^{0.7917})} \quad (5)$$

where I_m is the maximum LM-OSL intensity, t_m the time corresponding to I_m , λ the stimulation decay constant and R the re-trapping to recombination probabilities ratio.

2.3. Analytic equations for CW-OSL decay curve

CW-OSL, ITL equations

$$I(t) = \frac{I_m \lambda}{W(e^z) + W(e^z)^2} \quad (6)$$

$$z = \frac{R}{1-R} - \ln\left(\frac{1-R}{R}\right) + \frac{\lambda t}{1-R} \quad (7)$$

where all symbols have been previously explained.

2.4. Analytic OTOR dose response equation and the supra-linearity index $f(D)$

Dose response OTOR equation

$$I(D) = I_0 \left[1 + \frac{W\left((R-1) \cdot \exp\left((R-1) e^{-\frac{D}{D_c}}\right)\right)}{1-R} \right] \quad (8)$$

where $R = A_n/A_m$, with A_n the trapping coefficient, A_m the recombination coefficient and D_c the saturation dose of electron traps.

Supra-linearity index $f(D)$, OTOR

$$f(D) = \frac{1}{kD} \left(1 - \frac{W(z_1)}{R-1} \right) \quad (9)$$

where $z_1 = z_R \cdot e^{-D/D_c}$, $z_R = (R-1) \cdot e^{R-1}$ and $k = \frac{1}{(R-1)D_c} \cdot \frac{W(z_R)}{1+W(z_R)}$.

In all cases of aforementioned equations, I_o corresponds to the saturation intensity and the functions $W()$ and Ei are special functions contributing to all stimulated luminescence phenomena. For a detailed presentation see Section 3.1.

2.5. Analytic TTOR dose response equation and the supralinearity index $f(D)$

Researchers created the mixed order kinetics (MOK) model (Chen et al., 1981; Kitis and Gomez-Ros, 2000), which is a linear mixture of first and second order kinetics equations, to bridge the gap between these two aforementioned order of kinetics.

The analyzed Two Traps One Recombination center model (TTOR) describes superlinear dose response as a competition between two electron traps during a sample's irradiation stage.

Dose response TTOR equation

$$I(D) = I_0 \left[1 - \left(\frac{1}{B} W \left(B e^B e^{-\frac{D}{D_c}} \right) \right)^\alpha \right] \quad (10)$$

with $\alpha = \frac{A_2}{A_1}$, $B = \frac{N_1(A_1 - A_m)}{A_2 N_2 + A_m N_1}$ and D_c are free parameters depending on the values of trap populations and cross sections for trapping and recombination. In Eq. (10), for the case of TTOR model, the previously used parameter of the re-trapping coefficient of electrons (A_n ($\text{cm}^3 \text{s}^{-1}$)) is now clearly replaced by A_2 , and A_1 , referring to the two different traps, also those indexes have the same meaning for the other parameters accordingly (N_1 and N_2) (Wintle and Murray, 1997; Alexander and McKeever, 1998).

Supralinearity index $f(D)$, TTOR

$$f(D) = \frac{1}{kD} \left[1 - \left(\frac{W(z_2)}{B} \right)^\alpha \right] \quad (11)$$

where $z_2 = z_B \cdot e^{-D/D_c}$, $z_B = B \cdot e^B$ and $k = \left(\frac{1}{B} \right)^\alpha \frac{\alpha}{D_c} \cdot \frac{(W(z_B))^\alpha}{1+W(z_B)}$.

2.6. Goodness of fit

In order to determine if a fit is successful, the TL and OSL research community uses the Figure Of Merit (FOM%) indicator of Balian and Eddy (1977). It is given by the following expression:

$$FOM(\%) = 100 \cdot \sum_i \frac{|Y_{exp} - Y_{fit}|}{A} \quad (12)$$

where Y_{exp} is the experimental data, Y_{fit} is the theoretical data that results from the fitting and A is the area of the fitted curve.

3. Selection of programming language

All deconvolution and dose response fitting analysis were conducted in Python, with all required libraries used to generate the relevant scripts for each task. More specifically, Python is undoubtedly one of the most widely used and popular programming languages today, owing to its simple syntax, which emphasizes natural language like everyday English. Furthermore, the user has the option of selecting from a variety of libraries for mathematical analysis and data processing along with the proper documentation on how to use them. Python's popularity has resulted in a large community of Python users from whom one may get helpful advice on any script or lessons on how to get started with Python.

For the applications on the stimulated luminescence, Python offers a significant advantage compared to other computing environments. The Lambert $W()$, Wright Omega(), and Exponential integral $Ei()$ functions were previously included within the utilized libraries. This makes the analysis much less time consuming, as the users may use these functions at any moment in their script by just typing their name (for example, for the Lambert W function, simply typing `lambertw()` is required). Taking all the aforementioned into account, as well as Python's open-source licensing, Python is an excellent starting reference point for researchers

who are new with coding due to its user-friendly syntax and available support.

The scripts in this work use a plethora of libraries, including NumPy for editing n-dimensional tables, CSV for reading and writing csv files, SciPy.special to import the Lambert $W()$, Wright Omega(), and Exponential integral $Ei()$ functions, EasyGUI to create pop-up boxes, Pandas to handle data frames, Pybroom to "clean" data frames, and Matplotlib.plot to create plots.

The curve fit command from the SciPy.optimize sublibrary and the Lmfit library were used for optimization. Due to the fulfillment of the conditions for their use and their ability to produce very good fittings, three optimization methods from the LMfit library were used: Levenberg–Marquardt algorithm (a repetitive technique that tracks down the minimum of a multi-valued function that is expressed as the sum of squares of non-linear real-valued functions), Nelder–Mead simplex algorithm (generates a sequence of simplices to approximate an optimal point of $\text{minf}(x)$ and Powell's method (gradient-free minimization algorithm). All three methods were tested in order to compare the outcomes and determine which method was the most effective.

3.1. Special functions $W()$, $\omega()$ and $Ei()$

Python, Maple, MATLAB, Maxima, and Mathematica (Peng et al., 2021) contain, as said before, the Lambert $W()$ (equivalent the Wright Omega function) and the exponential integral function $Ei()$ as built-in functions like any other ordinary function. This allows the user to call each function purely by its name throughout the script. This built-in form of these functions makes all expressions used in the present work to be purely analytic.

As $e^z \rightarrow \infty$, $W(e^z)$ overflows. In this case, in the Python scripts $W()$ can be precisely approximated using the following expression (Peng et al., 2021):

$$W(e^z) = z - \ln(z) \quad (13)$$

Another way to avoid the overflow is to replace the $W(e^z)$, in all equations above, by the Wright $\omega()$ function by utilizing the relationship:

$$W(e^z) = \omega(z). \quad (14)$$

This is another advantage of Python, the co-existence of Lambert W and Wright Omega function as built-in functions. It must be noted, however, that the replacement of $W(e^z)$ with $\omega(z)$ holds only for the first real branch of the Lambert $W()$ function (Corless et al., 1996; Corless and Jeffrey, 2002)

3.2. Running the analysis program

The protocol for script run is shown in Fig. 2. In this Flowchart, there are two distinguished colors (light gray and pink) describing the process that the program follows in order to analyze the experimental data. The same procedure in terms of programming structure, is followed either for the deconvolution of stimulated luminescence signals (TL and OSL) or for fitting the dose response curves. In the back-end of the program there is a pre-written script, in which the appropriate libraries have been inserted, such as NumPy and SciPy among others. Following that, depending on the experimental phenomenon, the appropriate expressions have been defined in the form of functions in order to fit the experimental data based on the theoretical expressions. In order to ensure a good fit for the experimental measurements, it is essential that the Figure Of Merit (FOM %) should be as low as possible; FOM of 3% or lower is highly desirable. The other part that script follows (light pink color on the Flowchart) is the part of user's actions concerning the input of the data, the selection of the optimization method and the results of the analysis in the form of output files. This part of the program can be summarized as follows:

Table 1

Format of the file containing the initial values of all fitting parameters; the specific example corresponds to the deconvolution analysis of a TL glow curve.

Im, Tm, E, R	Min	Max
17302	16000	18000
337	273	304
0.9	0.3	2.5
0.028	0.00001	0.9
(empty line, 2nd peak)		
65678	64000	66000
391	273	400
1.25	0.3	2.5
0.008	0.00001	0.9
(empty line, <i>n</i> th peak)		

Table 2

File containing the fitting parameters of each peak for the case of TL deconvolution.

Peaks	Imax	Tmax	E	R	s	Total fom
0 Peak1	17302.32	337.859	0.972	0.029	3.04E+13	1.893
1 Peak2	65678.75	391.501	1.257	0.008	1.45E+15	
2 Peak3	64231.62	430.066	1.362	0.044	7.5E+14	
3 Peak4	72037.33	461.681	1.64	0	7.13E+16	
4 Peak5	192966.8	487.976	2.2	0.018	5.56E+21	

Input 1: A pop-up window prompts the user to enter the file holding the experimental data. This is a basic text file in tab-delimited format with three columns: the first column contains the numbering of experimental points, the second column includes the independent variable, and the third column contains the experimental values of *y* variable. The latter is always the luminescence signal; however for the cases of dose response curves it represents an integrated signal over an entire TL peak or OSL component. The independent *x*-variable could be (a) temperature (*K*) for the case of deconvolution of TL signal, (b) time (*s*) for deconvolving either CW- or LM-OSL curves and (c) dose (*Gy*) when fitting dose response curves. According to the type of data set and analysis required, the appropriate equation is selected.

Input 2: Then, the program asks the file in tab-delimited text format containing the initial values of the free parameters which are given by a file as that of Table 1 in the same pop-up box.

Input 3: A second pop-up window will appear, prompting the user to fill in the spaces with essential information when deconvolution of either TL glow curve or OSL decay curve is to be performed (number of peaks/components, initial values and range of kinetic parameters).

Input 4: Finally, from a third pop-up box the user will choose which optimization method he wants for the deconvolution/fitting process.

As shown, the user solely interacts with the script through a visual environment that includes instructions for each step. This implies that any user, regardless of programming experience, may work on these scripts.

When the program finishes the analysis, it creates a plot and the output files:

Output file 1: A file containing the analyzed data set (TL glow curve, OSL decay curve or Dose response) (Table 3).

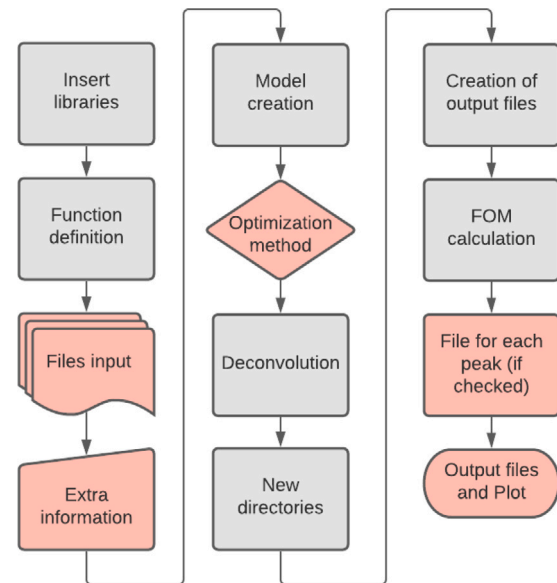
Output file 2: A file containing the values of all fitting parameters of each peak, component, response curve (Table 2).

Output file 3: (Optional) The user has the opportunity to create different files that contain the output results for each component separately through a fifth pop-up box.

Table 3

File containing the theoretical and experimental data of a glow curve.

<i>x</i>	Data	Best fit	Residual	Model (tl, prefix='t10')	...	
0	325	6502	9550.328	3048.328	9466.152	...
1	326	9346	10334.09	988.087	10237.471	...
2	328	11780	11961.24	181.238	11834.28	...
3	330	13538	13603.17	65.169	13436.897	...

**Fig. 2.** Flowchart of Python scripts.

4. Results and discussion

4.1. Deconvolution of various stimulated luminescence signals

In this section, specific examples of deconvolution analysis will be presented for the cases of TL glow curve, LM-OSL decay curve as well as CW-OSL decay curve. Therefore, the deconvolution results using the Lambert W function in the Python computing environment (hereafter approach **LW P**) will be compared to corresponding deconvolution analysis using (a) the Lambert W function in the Excel commercial spreadsheet (hereafter approach **LW E**, Konstantinidis et al., 2021), (b) the General Order Kinetic (GOK) in a commercial spreadsheet (hereafter approach **GOK**, Afouxenidis et al., 2011).

In the framework of the present study, three different minimizing algorithms were used and tested; the Nelder–Mead simplex algorithm, the Levenberg–Marquardt algorithm and the Powell simplex algorithm. The easy use of these minimizing approaches in Python computing environments stands as an alternative argument towards its application to stimulated luminescence. Table 4 presents all FOM values corresponding to the three different cases of stimulation moduli and all three minimizing approaches that were conducted. It is already known by the literature that the FOM should be lower than 2% in order for the deconvolution to be highly desirable. Generally, FOM values higher than 10% are strongly unpreferable, while those between 3% and 10% should be re-evaluated based on the deconvolution. As it can be observed in Table 4, in all cases FOM values range between 1.5 and 2, indicating that the deconvolution quality does not depend on the minimizing simplex approach. For the rest of the study, the Levenberg–Marquardt algorithm was adopted.

In order to check the applicability of the new deconvolution software in the case of TL, a TL glow curve of TLD 700 (LiF:Mg, Ti dosimeter manufactured by Harshaw Chemical Co., USA, with percentages 0,007% of ⁶Li and 99,993 of ⁷Li) was used. The reason

Table 4

FOM values corresponding to (a) TL, LM-OSL and CW-OSL curves and (b) to three different minimization algorithms. One single example for TL, LM-OSL and CW-OSL was fitted using all three minimization approaches. All curves included at least 1000 data points.

Phenomenon	FOM			Best method
	LM	NM	Powell	
TL	1.893%	1.794%	1.663%	LM
LM-OSL	1.498%	2.766%	1.246%	LM
CW-OSL	0.131%	0.131%	0.131%	NM

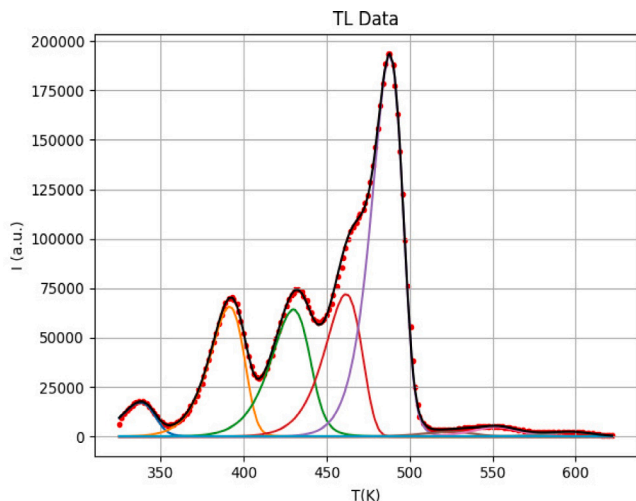


Fig. 3. Deconvolution of TL glow curve from TLD-700 sample using the LW P approach. Experimental data are presented as data points while continuous lines correspond to individual TL peaks and the total fit.

for this selection is multifold: (a) the corresponding TL glow curve is quite complex, consisting of several overlapping peaks, at least 8 within the temperature range between room temperature and 350 °C, (b) the TL glow curve of such dosimeter has been effectively deconvolved, not only in the voluminous literature but also from our group (Horowitz et al., 1979a, 1980; Kitis and Otto, 2000; Sadek et al., 2015; Konstantinidis et al., 2020), providing this experience, (c) the GLOCANIN project includes it as reference material for reference TL glow curves (Bos et al., 1993, 1994). Deconvolution analysis is presented in Fig. 3 while the corresponding fitting parameters are listed in Table 5; the same Table includes the deconvolution parameters of the other two approaches (LW E and GOK) for the sake of comparison. Specifically, all peaks seem to follow the first order kinetics and the activation energies are in alignment with those of the aforementioned literature (i.e. 1, 1.25, 1.35, 1.65 eV for peaks 1–4 and 2.2 eV for the known dosimetric peak 5 of TLD-700). As for the T_m values, there is no significant difference between the literature and the present study. Similarly to the experimental TL glow curve, all three approaches were used for deconvolving the reference TL glow curve RefGLOW009 of the GLOCANIN project (Bos et al., 1993, 1994). The results of the specific deconvolution analysis are presented in Fig. 4 and Table 6 in a similar way.

A closer look at Tables 5 and 6 will reveal an excellent agreement among the three different deconvolution approaches, especially when it comes to discuss the parameters T_m and E. This very good agreement is monitored in both cases of experimentally obtained TL glow curve of TLD 700 and RefGLOW009. Special care should be addressed while comparing the parameters of the order of kinetics, namely the R parameter in the case of the Lambert W function versus the b parameter in the GOK model. There is a one-to-one correlation between those two for the cases of (a) negligible re-trapping, where R takes values close or equal to 0 and b values close to 1 and (b) the case where the values

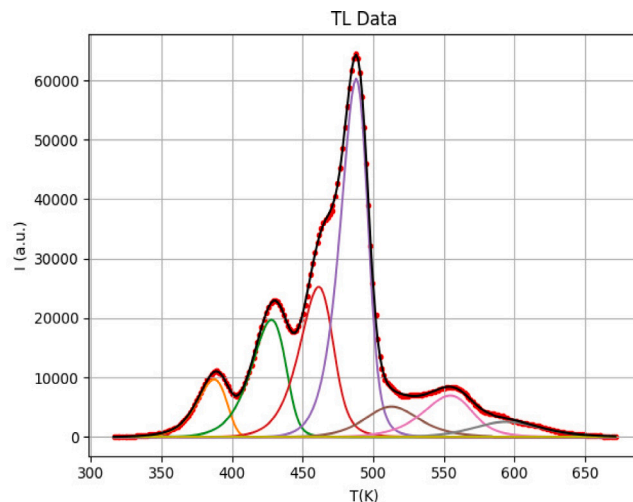


Fig. 4. As Fig. 3 for RefGLOW009 curve.

Table 5

Comparison of the calculated values of I_m , T_m , E and R parameters among different deconvolution approaches for the case of TLD 700. R is absent in the case of GOK, which uses the kinetic order parameter b.

	$I_m \cdot 10000$ (A.u.)		
	LW Python	LW Excel	GOK
P 1	1.7302	1.7265	1.7302
P 2	6.5679	6.5894	6.5679
P 3	6.4232	6.4558	6.4232
P 4	7.2037	7.1463	7.2037
P 5	19.2967	19.2330	19.2967
	T_m (K)		
	LW Python	LW Excel	GOK
P 1	338	338	337
P 2	392	392	392
P 3	430	430	430
P 4	462	462	461
P 5	488	488	488
	E (eV)		
	LW Python	LW Excel	GOK
P 1	0.97	0.97	0.98
P 2	1.26	1.26	1.26
P 3	1.36	1.36	1.36
P 4	1.64	1.64	1.63
P 5	2.20	2.20	2.20
	R (b for GOK)		
	LW Python	LW Excel	GOK
P 1	0.029	0.028	1.01
P 2	0.008	0.008	1.01
P 3	0.044	0.043	1.01
P 4	0.001	0.001	1.01
P 5	0.018	0.017	1.03

of b get close/equal to 2 and the values of R approach unity, indicating intense re-trapping. Both Tables suggest that in all cases, first order of kinetics describes all TL glow peaks.

Fig. 5 presents the corresponding deconvolution analysis on the LM-OSL signal for a quartz sample (from 0% to 90% of the maximum stimulation intensity of 40 mW/cm², light wavelength: 470 nm, stimulation duration P: 1000s, stimulation temperature: 25 °C) originated from Northern Greece (Koupa village, Polymeris et al., 2009). The deconvolution results of all three approaches are presented in Table 7. For the bell-shaped LM-OSL decay curve, the agreement among the parameters of the three deconvolution approaches is not so spectacular as for the case of TL. At first, minor divergence is monitored for the

Table 6

Comparison of the calculated values of I_m , T_m , E and R parameters among different deconvolution approaches for the case of RefGLOW009. R is absent in the case of GOK, which uses the kinetic order parameter b.

$I_m \cdot 10000$ (A.u.)			
	LW Python	LW Excel	GOK
P 2	0.9677	0.9811	0.9767
P 3	1.9735	1.9880	1.9622
P 4	2.5259	2.4564	2.3452
P 5	6.0256	6.1893	6.3303
T_m (K)			
	LW Python	LW Excel	GOK
P 2	387	387	387
P 3	427	428	428
P 4	461	461	460
P 5	488	488	488
E (eV)			
	LW Python	LW Excel	GOK
P 2	1.23	1.24	1.26
P 3	1.30	1.34	1.31
P 4	1.60	1.60	1.59
P 5	2.19	2.16	2.03
R (b for GOK)			
	LW Python	LW Excel	GOK
P 2	0.001	0.019	1.01
P 3	0.017	0.059	1.01
P 4	0.100	0.013	1.01
P 5	0.069	0.060	1.03

parameters of deconvolution parameters t_m and λ ; the values of these parameters differ almost as 10%–13%. Nevertheless, both parameters are included in the calculation of the photo-ionization cross section of each peak. It is quite apparent that these latter values stand in excellent agreement among the three deconvolution approaches. Nevertheless, the most prominent lack of agreement is yielded for the case of the order of kinetics. Despite the ubiquitous restriction for R, taking values being between 0.00001 and 1, it is quite important to remind that for the luminescence signals for quartz the first order of kinetics is dominant. In both cases where the R parameter is used, the minimizing procedure shows a tendency to prefer large values for this parameter. Similar features were also reported by Konstantinidis et al. (2021) for the case of the **LW E** approach. Unfortunately, for general order of kinetics, the values of R between 0.51 and 0.63 lie well beyond the region of first order of kinetics. Nevertheless, these values were approved by another scientific criterion for verifying the physical meaningfulness of the deconvolution procedure, arising from checking the values of the photo-ionization cross section for each LM-OSL component, according to the corresponding λ values (Konstantinidis et al., 2021). Since stimulated luminescence signals from quartz are described dominantly by first order of kinetics, in the deconvolution process the program shows a sensitivity in the initial values, so in order to avoid cases of second or even general order the R-parameter should be set close to R values depicting first order of kinetics.

Deconvolution analysis of CW-OSL decay curve seems to be more practical in terms of simplicity, as it involves one fitting parameter less for each component. Moreover, as Kitis and Pagonis (2008) have already argued, the resolution of a CW-OSL enables the use of maximum three decaying components. An example of deconvolution analysis for the CW-OSL signal from BeO (Aslar et al., 2019) is presented in Fig. 6. Table 8 presents the fitting parameters of all three deconvolution approaches. Agreement seems quite straightforward, even for the case of the R parameter describing the order of kinetics along with the re-trapping probability. The results of the present analysis stand in excellent agreement with previously reported results on BeO from Thermalox, where OSL is dominated by first order kinetics (Aslar et al., 2019).

Table 7

Comparison of t_m , R and λ parameters among three deconvolution approaches for the case of an LM-OSL of a quartz sample from Greece. Again, the GOK method "uses" the kinetic order b instead of R.

t_m (s)			
	LW Python	LW Excel	GOK
C 1	3.94	4.74	3.99
C 2	12.64	12.64	12.58
C 3	136.07	131.22	133.94
C 4	305.11	254.65	303.99
R (b for GOK)			
	LW Python	LW Excel	GOK
C 1	0.24	0.22	1.18
C 2	0.61	0.63	1.28
C 3	0.55	0.36	1.04
C 4	0.9	0.51	1.01
λ (s^{-1})			
	LW Python	LW Excel	GOK
C 1	15.527	10.688	13.480
C 2	1.654	1.698	1.730
C 3	0.020	0.013	0.022
C 4	0.003	0.004	0.004

Table 8

Comparison of λ and R (b for GOK) parameters among three deconvolution approaches for the case of an CW-OSL of a BeO sample.

λ (s^{-1})			
	LW Python	LW Excel	GOK
C 1	0.143	0.143	0.145
C 2	0.001	0.001	0.001
R (b for GOK)			
	LW Python	LW Excel	GOK
C 1	0.09	0.09	1.03
C 2	0.01	0.01	1.20

4.2. Dose response curves

In this section, specific examples of fitting analysis are presented for the cases of dose response curves with and without intense supralinearity. Therefore, the fitting results using the Lambert W function in the Python computing environment (**LW P** approach for dose response fitting) are compared to the corresponding dose response fitting analysis using solely the approach **LW E** (Konstantinidis et al., 2021). Both approaches were applied for both cases of dose response models, namely OTOR and TTOR; moreover, the supralinearity index $f(D)$ (Horowitz, 1981; Mische and McKeever, 1989) was also derived arithmetically according to the experimentally obtained dose response's data points and was further fitted independently using the corresponding equations. It is quite important to note that for a single dose response using the same model, the **LW P** approach results in two different, independently obtained sets of fitting parameters; one for the fitting analysis of the dose response and another corresponding to the fitting analysis of the supralinearity index $f(D)$.

Fig. 7a presents an example of dose response fitting analysis for the case of TL from $Al_2O_3:C$ grains while Fig. 7b depicts the corresponding analysis for the supralinearity index $f(D)$. Analysis was performed using the OTOR Eqs. (8) and (9) respectively. The corresponding model involves only three fitting parameters, the saturation intensity I_0 , the R parameter and of course the parameter D_c , corresponding to the dose that brings the system to saturation. Table 9 shows also the results from the corresponding analysis using the approach **LW E**. According to this Table, two important results can be revealed:

- The two fitting approaches (**LW P** and **LW E**) provide results with excellent agreement when applied to the same curve, namely either dose response or $f(D)$;

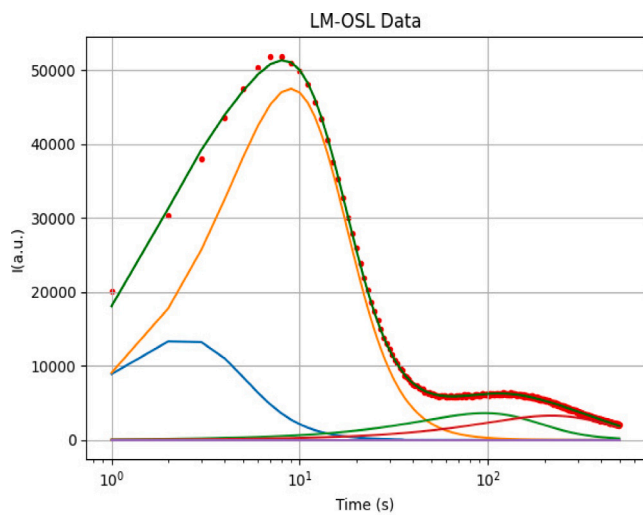


Fig. 5. Deconvolution of LM-OSL decay curve of Quartz originated from Koupa, Greece, using the LW P approach. Four individual components were used; these along with the final fit are presented as continuous lines, while data points correspond to experimental data.

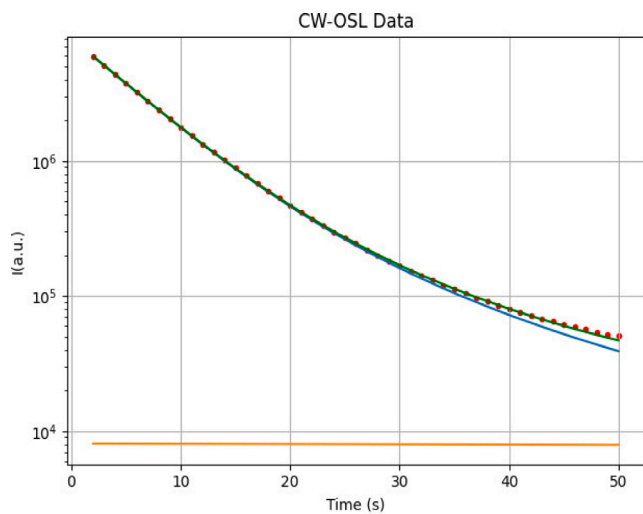


Fig. 6. Deconvolution of CW-OSL decay curve of BeO sample with the LW P approach, using 2 components. Experimental data are presented as points and the components along with the final fit as continuous lines.

b. Independent fitting of the dose response curve and the corresponding supralinearity index $f(D)$ for the same dataset results in different values for the fitting parameters D_c and R . This lack of agreement could be even of the order of 50%–75% and could be attributed to the presence of severe supralinearity effects, as it could be easily revealed by Fig. 7b.

Fig. 8a presents an example of simulated dose response that yields intense supralinearity (Nikiforov et al., 2014), while Fig. 8b shows the corresponding supralinearity index $f(D)$ versus dose; the dose response data of this latter are not experimental and were selected due to presence of strong supralinearity. Fitting analysis for both cases was performed using the TTOR Eqs. (10) and (11) respectively. The corresponding model involves one more fitting parameter compared to the corresponding OTOR model, namely the saturation intensity I_0 , the α parameter that corresponds to the relative population of the two traps, and of course the dose scaling constant D_c that has the same units as the dose; nevertheless, in this model it does not

Table 9

Comparison of the parameters D_c and R between the two methods using the Lambert W function (OTOR model) for a case of dose response, and the calculation of supralinearity index in $Al_2O_3:C$.

I(D)		
	LW Python	LW Excel
D_c	1043	1004
R	0.15	0.16
f(D)		
	LW Python	LW Excel
D_c	658	772
R	0.26	0.24

Table 10

Comparison of the parameters D_c , B and a between the two methods using the Lambert W function (TTOR model) for a case of dose response, and the calculation of supralinearity index in an anion-defective aluminum oxide single crystal.

I(D)		
	LW Python	LW Excel
D_c	0.08	0.07
B	3.12	3.55
a	0.05	0.03
f(D)		
	LW Python	LW Excel
D_c	0.07	0.07
B	7.45	8.27
a	0.14	0.11

represent the saturation dose. The last fitting parameter, denoted as B , is a dimensionless parameter that describes the competition ratio. Similar to all previous cases, the maximum intensity is not presented in Table 10, that shows the corresponding results from the corresponding analysis using both approaches $LW P$ and $LW E$. For all three different fitting parameters of the TTOR model, the same previous results (a & b) that were reported for the case of the OTOR model are also dominant, with one minor exception for the scaling constant D_c ; the latter is being constant, independent on (i) the fitting approach and (ii) whether the fitting analysis takes place on the dose response or the supralinearity index $f(D)$.

5. Conclusions

A new, flexible and versatile approach for mathematical formulation of stimulated luminescence phenomena includes the use of the Lambert W function in a computing environment developed in Python programming language. This approach was described for the first time in the literature within the present work. For the case of deconvolution analysis of stimulated luminescence signals, the specific approach works efficiently for TL and CW-OSL curves; nevertheless, fine tuning of the fitting constraints regarding the values of R parameter requires further work for the case of LM-OSL. For the case of dose response fitting analysis, this approach enables the easy application of non-empirical models towards increasing the accuracy of ages within the region of saturation; this increase in the precision is feasible as the use of Lambert W function will decrease substantially the error of the equivalent dose calculation within the saturation region. Further work is required in order to better comprehend the physical meaning in the selection of fitting parameters. Simultaneous fitting of both dose response and supralinearity index $f(D)$ curves might result in better understanding of both competition as well as non-linear effects. Taking into account that Python is an accessible tool for every researcher with a vast number of libraries to use as well as a huge repository of examples, it is an excellent tool for stimulated luminescence curve deconvolution and fitting analysis.

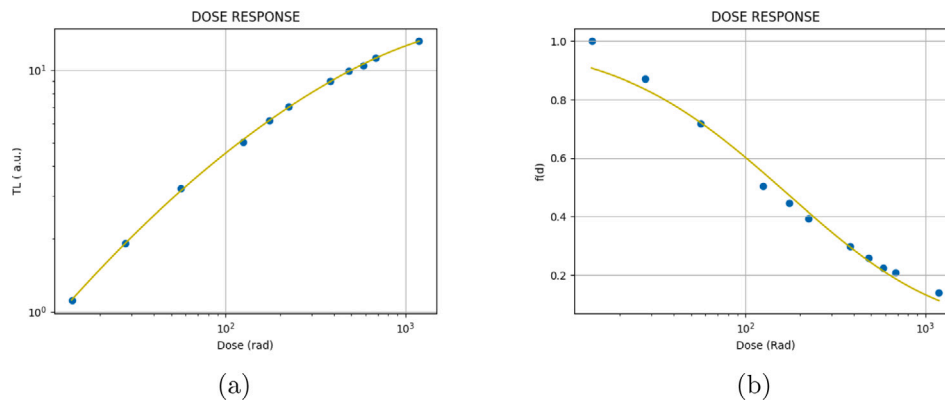


Fig. 7. (a) Analysis of a TL dose response curve of the main dosimetric peak (150–230 °C) of $\text{Al}_2\text{O}_3 : \text{C}$ at room temperature and (b) its supralinearity index with the OTOR model.

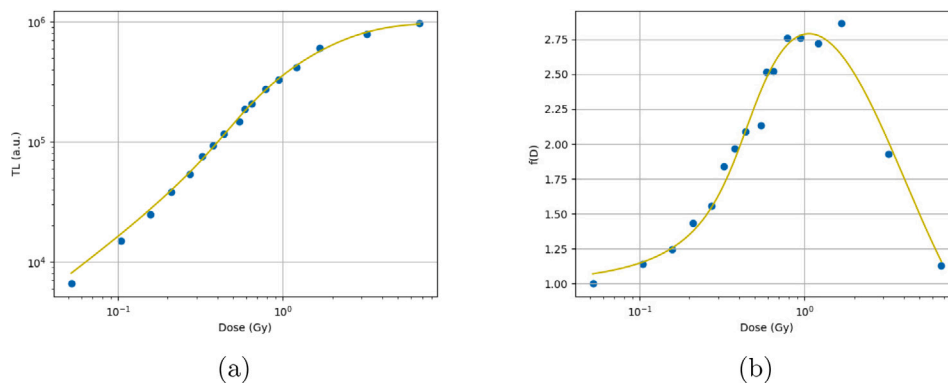


Fig. 8. Analysis of a dose response curve (a) and the corresponding supralinearity index (b) of an anion-defective aluminum oxide single crystal based on the TTOR model, using the LW P approach. (Nikiforov et al., 2014).

6. Sharing the scripts

The scripts, along with documentation on how to use them, are available on GitHub (<https://github.com/kpreveza/Stimulated-Luminescence>).

Declaration of competing interest

The authors declare that they have no known competing financial interests or personal relationships that could have appeared to influence the work reported in this paper.

References

- Afouxenidis, D., Polymeris, G.S., Tsirliganis, N.C., Kitis, G., 2011. Computerized curve deconvolution of TL/OSL curves using a popular spreadsheet program. *Radiat. Prot. Dosim.* 149, 363–370.
- Alexander, C.S., McKeever, S.W.S., 1998. Phototransferred thermoluminescence. *J. Phys. Appl. Phys.* 31, 2908–2920.
- Aslar, E., Meriç, N., Sahiner, E., Erdem, O., Kitis, G., Polymeris, G.S., 2019. A correlation study on the TL, OSL and ESR signals in commercial BeO dosimeters yielding intense transfer effects. *J. Lumin.* 214, 116533.
- Balian, H.G., Eddy, W., 1977. Figure-of-merit (FOM), an improved criterion over the normalized Chi-squared test for assessing goodness-of-fit of Gamma-ray spectral peaks. *Nucl. Instrum. Methods* 2389–2395.
- Bos, A.J.J., Piters, T.M., Gomez-Ros, J.M., Delgado, A., 1993. An intercomparison of glow curve analysis computer programs I. Synthetic glow curves. *Radiat. Prot. Dosim.* 47, 473–477.
- Bos, A.J.J., Piters, T.M., Gomez-Ros, J.M., Delgado, A., 1994. An intercomparison of glow curve analysis computer programs II. Measured glow curves. *Radiat. Prot. Dosim.* 51, 257–264.
- Chen, R., Kristianpoller, N., Davidson, Z., Visocekas, R., 1981. Mixed first and second order kinetics in thermally stimulated processes. *J. Lumin.* 23 (3–4), 293–303.
- Corless, R., Gonnet, G., Hare, D., Jeffrey, D., 1996. On the Lambert W function. *Adv. Comput. Math.* 5, 329–359. <http://dx.doi.org/10.1007/BF02124750>.
- Corless, R., Jeffrey, D., 2002. The wright ω function. *Artif. Intell.* 76–89. <http://dx.doi.org/10.1007/3-540-45470-5-10>.
- Horowitz, Y.S., 1981. The theoretical and microdosimetric basis of thermoluminescence and applications to dosimetry. *Phys. Med. Biol.* 26 (5), 765.
- Horowitz, Y.S., Fraier, I., Kalef-Ezra, J., Pinto, H., Goldbart, Z., 1979a. *Phys. Med. Biol.* 24, 1268–1275.
- Horowitz, Y.S., Kalef-Ezra, J., Moscovitch, M., Pinto, H., 1980. *Methods* 172, 479–485.
- Kitis, G., Gomez-Ros, J.M., 2000. Thermoluminescence glow-curve deconvolution functions for mixed order of kinetics and continuous trap distribution. *Nucl. Instrum. Methods Phys. Res. A* 440 (1).
- Kitis, G., Gomez-Ros, J.M., Tuyn, J.W.N., 1998. Thermoluminescence glow-curve deconvolution functions for first, second and general orders of kinetics. *J. Phys. Appl. Phys.* 31 (19), 2636–2641.
- Kitis, G., Otto, T., 2000. *Nucl. Instrum. Methods B* 160, 262–273.
- Kitis, G., Pagonis, V., 2008. Computerized curve deconvolution analysis for LM-OSL. *Radiat. Meas.* 43, 737–741.
- Kitis, G., Polymeris, G.S., Pagonis, V., 2019. Stimulated luminescence emission: From phenomenological models to master analytical equations. *Appl. Radiat. Isot.* 153, 108797.
- Kitis, G., Vlachos, N.D., 2013. General semi analytical expressions for TL, OSL and other luminescence stimulation modes derived from the OTOR model using the Lambert W-function. *Radiat. Meas.* 48, 47–54.
- Konstantinidis, P., Kioumourtzoglou, S., Polymeris, G.S., Kitis, G., 2021. Stimulated luminescence; Analysis of complex signals and fitting of dose response curves using analytical expressions based on the Lambert W function implemented in a commercial spreadsheet. *Appl. Radiat. Isot.* 176 (2021), 109870.
- Konstantinidis, P., Tsoutsoumanos, E., Polymeris, G.S., Kitis, G., 2020. Thermoluminescence response of various dosimeters as a function of irradiation temperature. *Radiat. Phys. Chem.* 109156.
- Mische, E.F., McKeever, S.W.S., 1989. Mechanisms of supralinearity in Lithium fluoride thermoluminescence dosimeters. *Radiat. Prot. Dosim.* 29, 159–175.
- Nikiforov, S.V., Kortov, V.S., Kazantseva, M.G., 2014. Simulation of the superlinearity of dose characteristics of thermoluminescence of anion defective aluminum oxide. *Phys. Solid State* 56 (3), 554–560.

- Pagonis, V., 2021. *Luminescence: Data Analysis and Modeling using R*, Use R. Springer, Cham.
- Pagonis, V., Kitis, G., Chen, R., 2020a. A new analytical equation for the dose response of dosimetric materials, based on the Lambert W function. *J. Lumin.* 225, 117333.
- Pagonis, V., Kitis, G., Chen, R., 2020b. Superlinearity revisited: A new analytical equation for the dose response of defects in solids, using the Lambert W function. *J. Lumin.* 117553.
- Peng, J., Sadek, A.M., Kitis, G., 2021. New analytical expressions derived from the localized transition model for luminescence stimulation modes of TL and LM-OSL and their applications in computerized curve deconvolution. *Nucl. Instrum. Methods Phys. Res. B* 507, 46–57.
- Polymeris, G.S., Afouxenidis, D., Tsirliganis, N.C., Kitis, G., 2009. The TL and room temperature OSL properties of the glow peak at 110 °C in natural milky quartz: A case study. *Radiat. Meas.* 44 (1), 23–31.
- Sadek, A.M., Eissa, H.M., Basha, A.M., Carinou, E., Askounis, P., Kitis, G., 2015. *Radiat. Isot.* 95, 214–221.
- Sadek, A.M., Eissa, H.M., Basha, A.M., Kitis, G., 2014a. Development of the peak fitting and peak shape methods to analyze the thermoluminescence glow-curves generated with exponential heating function. *Nucl. Instrum. Methods Phys. Res. B* 330, 103–107.
- Sadek, A.M., Eissa, H.M., Basha, A.M., Kitis, G., 2014b. Resolving the limitation of the peak fitting and peak shape methods in the determination of the activation energy of thermoluminescence glow peaks. *J. Lumin.* 146, 418–423.
- Singh, L.L., Gartia, R.K., 2013. Theoretical derivation of a simplified form of the OTOR/GOT differential equation. *Radiat. Meas.* 59, 160–164.
- Singh, L.L., Gartia, R.K., 2015. Derivation of a simplified OSL OTOR equation using Wright Omega function and its application. *Nucl. Instrum. Methods Phys. Res. B* 346, 45–52. <http://dx.doi.org/10.1016/j.nimb.2015.01.038>.
- Wintle, A.G., Murray, A.S., 1997. The relationship between quartz thermoluminescence, photo-transferred thermoluminescence, and optically stimulated luminescence. *Radiat. Meas.* 27 (4), 611–624.